ELSEVIER

Materials and Engineering B103 (2003) 122–127

MATERIALS SCIENCE & ENGINEERING B

www.elsevier.com/locate/mseb

Electronic band-structure engineering of GaAs/$Al_xGa_{1-x}As$ quantum well superlattices with substructures

Mingrong Shen [a,b,*], Wenwu Cao [a,c]

[a] *Materials Research Institute, The Pennsylvania State University, University Park, PA 16802, USA*
[b] *Department of Physics, Suzhou University, Suzhou 215006, China*
[c] *Department of Mathematics, The Pennsylvania State University, University Park, PA 16802, USA*

Received 18 September 2002; received in revised form 22 April 2003; accepted 5 May 2003

Abstract

We report a theoretical investigation on the band structures of electrons in both infinite and finite semiconductor quantum well/barrier superlattices with each unit cell containing alternately two types of materials. When the unit cell of a superlattice, made of GaAs and $Al_xGa_{1-x}As$, is further divided into four and six sublayers of these two materials, narrower passbands and/or broad stopbands can be obtained for electrons with energy slightly larger than the potential barrier. When a finite superlattice has two different periods and each unit cell contains six sublayers of alternating GaAs and $Al_xGa_{1-x}As$, very sharp passbands can be obtained for electron energy right below and above the potential barrier. The results may be used to build a high-Q electron energy filter.

Keywords: Band structure calculations; Electron states; Gallium arsenide

PACS numbers: 73.20.Dx; 73.20.At; 61.72.Vv; 71.90.+q

1. Introduction

Advances in the growth technology of semiconductors have made it possible to fabricate complicated semiconductor microstructures, which can be used to regulate the motion of electrons. In particular, one-dimensional semiconductor superlattices consisting of alternating ultrathin layers of different composition or different levels of doping have been obtained using molecular beam epitaxy (MBE) and metal-organic chemical vapor deposition (MOCVD). The thickness of the layers is on the scale of the de Broglie wavelength of an electron. One of the motivations to study semiconductor superlattices lies in their possible applications as new devices, for example, electron energy filter, because the electronic responses of such devices can be tailored by varying the composition and thickness of these layers [1,2]. Due to the relatively longer mean free path of the electrons compared with the spacing of the semiconductor superlattices, electrons moving in a semiconductor superlattice can experience many periods before loosing their phase coherence. As a result, superlattice minibands can be formed, which superimpose onto the conduction and valence bands of the host semiconductor materials.

The electronic, transport, and optical properties of periodic and aperiodic semiconductor superlattices have been systematically studied, both experimentally and theoretically [3–9]. However, most of the reported works on periodic semiconductor superlattices were focused on layered structures consisting of only two sublayers in one unit cell. The aim of present work is to investigate theoretically the changes of the dispersion relations in infinite semiconductor superlattices and the transmission coefficient of electron waves in finite periodic superlattice structures with each unit cell containing several sublayers of the two materials. We also use finite size superlattices of multiple periodicities to regulate the mini-band-structure, analogous to our

* Corresponding author.
E-mail address: mrshen@suda.edu.cn (M. Shen).

0921-5107/03/$ - see front matter
doi:10.1016/S0921-5107(03)00159-4

recent study on acoustic bandgap engineering [10], but the unique quantum resonance tunneling effects of electrons bring some new and interesting physics into the superlattice problem. The theoretical study was carried out mainly within the framework of the Kronig–Penny (KP) model [11] and the use of the transfer matrix method. Although first principles calculations of superlattice structure, which use quantum theory for electrons by including many-body interactions, can be more accurate than calculations based on the KP model, the computations involved is very intensive and limited to a few unit cells [12]. On the other hand, for potential barrier thickness greater than 20 Å, the KP model is a reasonable approximation for the calculation of band structures of non-interaction electrons in infinite semiconductor superlattices [13].

In Section 2, the dispersion relations of electrons in infinite periodic semiconductor superlattices with each unit cell contains several sub-layers of two kinds of materials are derived. We use the GaAs/$Al_xGa_{1-x}As$ semiconductor superlattice as an example with each unit cell containing alternatingly two, four and six sublayers, respectively, of GaAs and $Al_xGa_{1-x}As$ of different thickness. Transmission coefficients were studied for cases with the electron energy both below and above the barrier height. In Section 3, we introduce an extension to the transfer matrix technique, which enables us to calculate the band structures of finite size superlattice without using the Bloch theorem. The transmission coefficient was calculated as a function of electron energy. In Section 4, a special structure of superlattice with two sub-periodic-structures is studied, which can be used as high-Q electron energy filter with extremely narrow passbands. Section 5 contains the summary and conclusions.

2. Dispersion relations for infinite semiconductor superlattice

First, we consider an infinite semiconductor superlattice made of two different materials X and Y. Each unit cell contains M layers of X and Y with different thickness, and we use $(X_1Y_1X_2Y_2—X_MY_M)_n$ to represent the nth unit cell. The thickness of these layers are d_{X1}, d_{Y1}, d_{X2}, d_{Y2}, …, d_{XM}, d_{YM}, respectively. These layers form quantum wells/barriers for the electron waves as depicted in Fig. 1.

When an electron with energy above the potential barrier V_0 is incident normal to the layered structure, the wave function at the jth layer of the nth cell can be written in the following form by solving the Schrodinger's equation:

$$\Psi_{n,j} = a_{n,j}\, e^{-ik_j z} + b_{n,j}\, e^{-ik_j z} \tag{1}$$

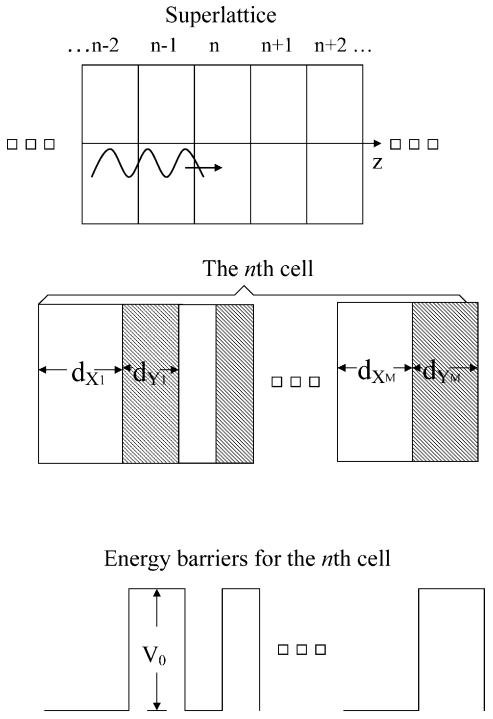

Fig. 1. Illustration of a superlattice and its M-layer unit cell with materials X and Y in alternating positions. The corresponding potential well/barrier structure is also depicted.

where n is the unit cell number, and j is the layer number within the nth cell. The first term on the right hand side of Eq. (1) represents the forward wave and the second term represents the reflecting wave, and k_j is the wave vector for electron propagating in the jth material given by:

$$\frac{\hbar k_X^2}{2m_X} = \varepsilon \quad \text{(in material } X\text{)} \tag{2}$$

$$\frac{\hbar k_Y^2}{2m_Y} = \varepsilon - V_0 \quad \text{(in material } Y\text{)} \tag{3}$$

where ε is the energy of the electron measured from the potential level of material A (bottom of the well), and m_X amd m_Y are the electron effective masses in X and Y, respectively. Note that k_Y becomes pure imaginary when $\varepsilon < V_0$. This case represents the situation inside the energy barrier and the wave function Eq. (1) becomes exponential functions without wave characteristics. Interestingly, resonance tunneling will occur for such situation as discussed below. For the superlattice of GaAs/$Al_xGa_{1-x}As$, the relation between the effective masses and the Al content x is [13]:

$$m_X = 0.067_{m_0}, \qquad m_Y = (0.067 + 0.083x)m_0 \tag{4}$$

where m_0 is the bare electron mass. By applying the appropriate boundary conditions at the interface between materials X and Y we have [14,15]:

$$\psi_X|_{\text{boundary}} = \psi_Y|_{\text{boundary}},$$

$$\frac{1}{m_X}\frac{\partial \psi_X}{\partial z}|_{\text{boundary}} = \frac{1}{m_Y}\frac{\partial \psi_Y}{\partial z}|_{\text{boundary}}. \quad (5a, b)$$

The continuity equations Eq. (5a,b) leads to the following relations among the coefficients $a_{n,l}$, $b_{n,l}$ and $a_{n+1,l}$, $b_{n+1,l}$ for two adjacent cells

$$\begin{pmatrix} a_{n,l} \\ b_{n,l} \end{pmatrix} = \begin{pmatrix} A & B \\ C & D \end{pmatrix} \begin{pmatrix} a_{n+1,l} \\ b_{n+1,l} \end{pmatrix} \quad (6)$$

where the 2×2 transfer matrix is given by:

$$\begin{pmatrix} A & B \\ C & D \end{pmatrix} = \prod_{j=1}^{M} \begin{pmatrix} A_j & B_j \\ C_j & D_j \end{pmatrix} \quad (7)$$

with

$$A_j = \frac{w_j + w_{j+1}}{2w_j} e^{i(k_j - k_{j+1})z_j}$$

$$B_j = \frac{w_j - w_{j+1}}{2w_j} e^{i(k_j + k_{j+1})z_j}$$

In Eq. (7) C_j and D_j are the complex conjugates of B_j and A_j, respectively, z_j is the coordinate of the interface between the jth and $(j+1)$th layers, and $w_j = k_j/m_j$, which is imaginary if the electron energy is less than the barrier height.

According to the Bloch theorem, for an infinite superlattice, the coefficients $a_{n,j}$ and $b_{n,j}$ for the same material in different unit cells must be the same except a phase shift and can be expressed as:

$$\begin{pmatrix} a_{n,j} \\ b_{n,j} \end{pmatrix} = \begin{pmatrix} a_{n+1,j} \\ b_{n+1,j} \end{pmatrix} e^{-ikd} \quad (8)$$

where k is the Bloch wave vector defined over the first Brillion zone ($-\pi/d < k \le \pi/d$), and d is the period of a unit cell.

The dispersion relation can be obtained from equation Eqs. (6) and (8),

$$k = \frac{1}{d} \arccos\left[\frac{1}{2}(A + D)\right] \quad (9)$$

where

$$\begin{aligned} A + D = & \prod_{h=1}^{M} \cos(k_h d_h) \\ & - \sum_{h=1}^{M-1} \times \sum_{j=h+1}^{M} \left[\left(\frac{w_h}{w_j} + \frac{w_j}{w_h}\right) \sin(k_h d_h)\sin(k_j d_j) \times \prod_{l(\neq h,j)=1}^{M} \cos(k_l d_l)\right] \\ & + \sum_{h=1}^{M-3} \sum_{j=h+2}^{M-1} \sum_{k=h+1}^{j-1} \times \sum_{l=j+1}^{M} \left[\left(\frac{w_h w_j}{w_l w_k} + \frac{w_l w_k}{w_h w_j}\right) \sin(k_h d_h)\sin(k_j d_j)\sin(k_k d_k)\sin(k_l d_l) \times \prod_{n(\neq h,j,k,l)=1}^{M} \cos(k_n d_n)\right] \\ & - \sum_{h=1}^{M-5} \sum_{j=h+2}^{M-3} \sum_{k=h+4}^{M-1} \sum_{l=h+1}^{j-1} \sum_{m=j+1}^{k-1} \times \sum_{n=k+1}^{M} \left[\left(\frac{w_h w_j w_k}{w_l w_m w_n} + \frac{w_l w_m w_n}{w_h w_j w_k}\right) \sin(k_h d_h)\sin(k_j d_j)\sin(k_k d_k) \right. \\ & \left. \sin(k_l d_l)\sin(k_m d_m)\sin(k_n d_n) \prod_{q(\neq h,j,k,l,m,n)=1}^{M} \cos(k_q d_q)\right] \\ & + \sum_{h=1}^{M-7} \sum_{j=h+2}^{M-5} \sum_{k=h+4}^{M-3} \sum_{l=h+6}^{M-1} \sum_{m=h+1}^{j-1} \sum_{n=j+1}^{k-1} \sum_{p=k+1}^{l-1} \times \sum_{q=l+1}^{M} \left[\left(\frac{w_h w_j w_k w_l}{w_m w_n w_p w_q} + \frac{w_m w_n w_p w_q}{w_h w_j w_k w_l}\right) \right. \\ & \left. \sin(k_h d_h)\sin(k_j d_j)\sin(k_k d_k)\sin(k_l d_l) \right. \\ & \left. \sin(k_m d_m)\sin(k_n d_n)\sin(k_p d_p)\sin(k_q d_q) \prod_{s(\neq h,j,k,l,m,n,p,q)=1}^{M} \cos(k_s d_s)\right] - \ldots\ldots \end{aligned} \quad (10)$$

where the subscripts h, j, k, l, m, n, p, q, r, and s are all integers. When there are 2, 4, and 6 sublayers in a unit cell, Eq. (10) is truncated at the second, third and fourth terms, respectively. Equation (10) is valid for $\varepsilon \ge V_0$ where k_Y is real. When $\varepsilon < V_0$, $k_Y = i\,k'_Y$ is pure imaginary, the above equation is still valid if the following relations are used:

$$\sin(k_Y d_Y) = i \sinh(k'_Y d_Y)$$
$$\cos(k_Y d_Y) = \cosh(k'_Y d_Y) \quad (11)$$

The calculated dispersion relations for electrons (of energy larger than V_0) propagating through infinite superlattice with each cell containing two, four or six layers of alternating GaAs and $Al_{0.3}Ga_{0.7}As$ are shown in Fig. 2. In each case, the volume ratio of GaAs and $Al_{0.3}Ga_{0.7}As$ was kept constant so that the cell period is kept at $d = 18$ nm. Fig. 2(a) is a typical dispersion relation for an infinite semiconductor superlattice formed by two sublayer unit cells. The piecewise

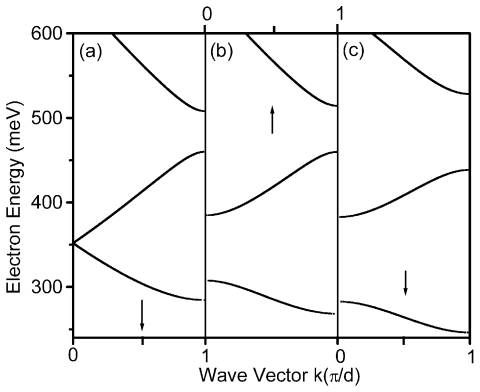

Fig. 2. Dispersion relations for infinite GaAs/$Al_{0.3}Ga_{0.7}As$ superlattices with multilayer unit cell. The electron energy is above the barrier height of $V_0 = 240$ meV. (a) Two sublayers in one unit cell with $d_{X1} = 12$ nm, and $d_{Y1} = 6$ nm. (b) Four sublayers in one unit cell with $d_{X1} = 7$ nm, $d_{Y1} = 3$ nm, $d_{X2} = 5$ nm, and $d_{Y2} = 3$ nm. (c) Six sublayers in one unit cell with $d_{X1} = 2$ nm, $d_{Y1} = 2$ nm, $d_{X2} = 4$ nm, $d_{Y2} = 2$ nm, $d_{X3} = 6$ nm, and $d_{Y3} = 2$ nm.

dispersion curves represent the passbands and the gaps are the stopbands. If the unit cell is subdivided into four sublayers of alternating GaAs and $Al_{0.3}Ga_{0.7}As$, flatter passbands and wider stopbands are formed. This trend is confirmed by further subdividing the unit cell into six layers of alternating GaAs and $Al_{0.3}Ga_{0.7}As$ as shown in Fig. 2(c). It is also noted that the first passband shifts down to lower energy when the unit cell is divided into more sublayers. Fig. 3 corresponds to the case when the electron energy is lower than the barrier height V_0. Other parameters are the same as for the case shown in Fig. 2. In this case, the first passband moves to higher energy when the unit cell is changed from two sublayers to four and six sublayers. The first three passbands get closer as the unit cell is divided into four and six layers while the shape of the pass bands does not change significantly. The stopbands also have some changes, however, far less noticeable as for the case shown in Fig. 2.

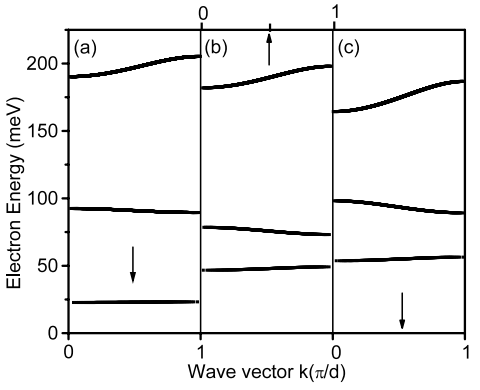

Fig. 3. The dispersion curves for the case shown in Fig. 2 with the electron energy blow the barrier height V_0. All parameters are the same as given in the caption of Fig. 2.

The Bloch theorem is only valid for an infinite system for which periodic condition holds. This does not reflect real experimental situations since the measured structures are always finite in size. Band structures are incomplete for a finite system although the shape could be similar to that of the infinite system, therefore, it is more meaningful to study the frequency spectrum of the transmission coefficient for finite systems.

3. Energy spectrum of the transmission coefficient for finite size superlattices

Considering a finite system of N cells, we can derive the following relation, according to the recurrence relation Eq. (6):

$$\begin{pmatrix} a_{1,1} \\ b_{1,1} \end{pmatrix} = [\mathrm{T}] \begin{pmatrix} a_{N+1,1} \\ b_{N+1,1} \end{pmatrix} \tag{12}$$

where the T matrix in Eq. (12) is a second rank tensor given by:

$$[\mathrm{T}] = \prod_{n=1}^{N} \begin{pmatrix} A_n & B_n \\ C_n & D_n \end{pmatrix}. \tag{13}$$

Assuming the electron is incident from the left (GaAs), only a transmitted wave exists in the right hand side of the superlattice (also GaAs), that is $b_{N+1,1} = 0$.

Now let us define a transmission function $\mathrm{H}(\varepsilon)$, analogous to acoustic waves in one dimensional finite periodic structures [16],

$$\mathrm{H}(\varepsilon) = \frac{a_{N+1,1}}{a_{1,1}}\, \mathrm{e}^{-ik_X Nd} = \frac{1}{T_{11}}\, \mathrm{e}^{-ik_X Nd}, \tag{14}$$

which describes both the amplitude and phase relationships between the incident electron wave at $z = 0$ and the transmitted wave at $z = Nd$. The transmission coefficient is given by:

$$t = H(\varepsilon) \cdot H^*(\varepsilon) \tag{15}$$

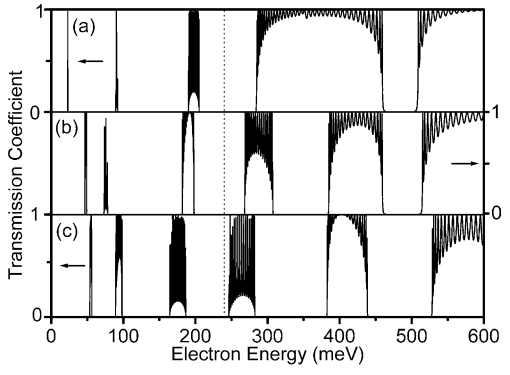

Fig. 4. Calculated energy spectrum of the transmission coefficient for finite size superlattices ($N = 20$). (a) Two sublayers, (b) four sublayers and (c) six sublayers. The corresponding parameters used for the calculations are the same as those given in Fig. 2.

Fig. 4 shows the calculated energy spectra of the transmission coefficient for one unit cell containing two, four and six layers of alternating GaAs and $Al_{0.3}Ga_{0.7}As$. The total number of cells is 20 for this calculated structure. Other parameters used are the same as for the case given in Fig. 2. The band ranges are consistent with that of Figs. 2 and 3, therefore, the definition of the transmission coefficient is appropriate. We found that sharp passbands and wider stopbands could be obtained when the unit cell was divided into more sublayers. Gipps-type oscillations were seen in the passbands, which come from the finite nature of the system. Complete transmission, i.e. $t=1$, can be achieved at isolated energies due to the resonance nature of the electron wave. The stopbands corresponds to total reflection, i.e. $t=0$. For a finite system, such condition cannot be achieved, but the value of t can become negligibly small as N increases. Resonance tunneling can occur for multiple periodic barriers and the passbands are much narrower compared with the passbands above the energy barrier.

The bandgaps can also be adjusted through changing the volume ratio of GaAs and $Al_xGa_{1-x}As$. In Fig. 5, we showed the effects where the total barrier thickness is increased. The ratios of total thickness of the barriers to that of the wells in one unit cell are, respectively, 0.5 [Fig. 5(a)], 1.0 [Fig. 5(b)], and 2.0 [Fig. 5(c)]. It can be seen that narrower passbands can be obtained when the ratio increases, and the passbands also shift to higher energies both below and above the barrier height V_0.

Because the mean free path of the electrons is finite, numerical calculations for a finite number of periods are more meaningful. On the other hand, our study indicated that a finite number of cells could already support a well-defined band structures.

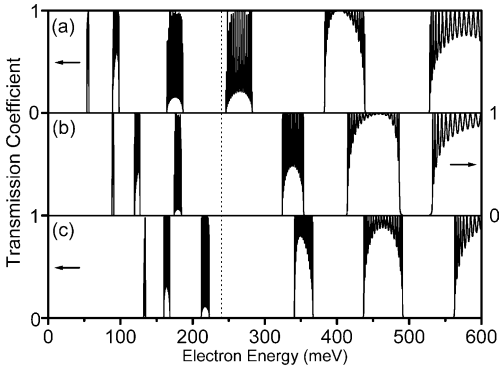

Fig. 5. Change of energy spectrum of the transmission coefficient for a finite superlattice ($N=20$) with six sublayers in one unit cell. The volume ratios of $Al_{0.3}Ga_{0.7}As$ are: (a) 1/3; (b) 1/2 and (c) 2/3, respectively. The corresponding thickness of each sublayer is given by: (a) $d_{X1}=2$ nm, $d_{Y1}=2$ nm, $d_{X2}=4$ nm, $d_{Y2}=2$ nm, $d_{X3}=6$ nm, and $d_{Y3}=2$ nm. (b) $d_{X1}=2$ nm, $d_{Y1}=3$ nm, $d_{X2}=3$ nm, $d_{Y2}=3$ nm, $d_{X3}=4$ nm, and $d_{Y3}=3$nm. (c) $d_{X1}=2$ nm, $d_{Y1}=2$ nm, $d_{X2}=2$ nm, $d_{Y2}=4$ nm, $d_{X3}=2$ nm, and $d_{Y3}=6$ nm.

4. A finite superlattice with two periodic substructures

We consider a finite superlattice containing two substructures of different periods. The main objective here is to use the idea of band-gap engineering to fabricate quantum well/barrier structures that have very narrower passbands for filter applications. Each substructure of the superlattice can produce its own band structure as discussed in previous section. If the passbands of the two substructures are not overlapped in certain energy range, the probability for the electron to pass through the whole structure will be low, which creates a broader stopband; if they are partially overlapped, only the overlapped part of energy band allow electrons to pass, thus, a narrow band electron energy filter is obtained.

The condition to realize the above idea is that both superlattices should have relatively broad stopbands to begin with. The results in Section 3 shows that we can use the superlattice with unit cell containing six sublayers of alternating GaAs and $Al_xGa_{1-x}As$ to obtain broad stopbands in the electron energy range above V_0 ($=240$ meV in our calculation). Fig. 6 shows the calculated energy spectrum of the transmission coefficient for the superlattices containing two different subsuperlattices. Each substructure has 20 unit cells so that the whole structure contains 40 cells in total. It is interesting to see that two very narrow passbands centered at about 163 and 437 meV, respectively, were indeed obtained in the energy ranges slightly below and slightly above V_0. As the electron energy increases, the effects of the barriers become weaker. When the electron energy is more than two times higher than the barrier height, $\varepsilon > 2V_0$, the superlattice idea cannot be used to design energy filter since the stop bands are very narrow to begin with as shown in Fig. 4 for the electron energy greater than 500 meV.

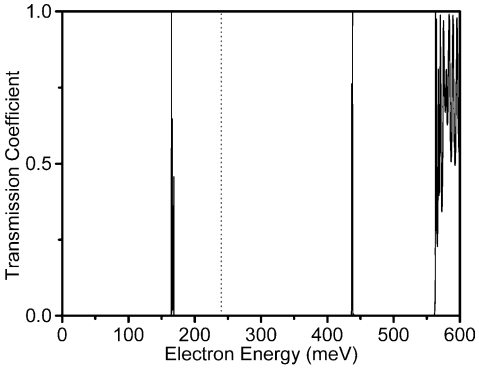

Fig. 6. Calculated energy spectrum of the transmission coefficient for a superlattice structure containing two sub-superlattices. The thickness values in one of the superlattices are: $d_{X1}=2$ nm, $d_{Y1}=2$ nm, $d_{X2}=4$ nm, $d_{Y2}=2$ nm, and $d_{X3}=6$ nm, $d_{Y3}=2$ nm; and in the other type of cells are: $d'_{X1}=2$ nm, $d'_{Y1}=2$ nm, $d'_{X2}=2$ nm, $d'_{Y2}=4$ nm, $d'_{X3}=2$ nm, and $d'_{Y3}=6$ nm.

5. Summary and conclusions

Electronic bandgaps produced by semiconductor superlattices stem from the wave characteristics of electrons. In this paper, we have investigated two types of superlattices and their associated energy band structures. The first is a quantum well/barrier superlattice with each unit cell containing several sublayers of two materials in alternate positions. Numerical calculations of the dispersion relation for an infinite superlattice and transmission coefficient for a finite GaAs/$Al_xGa_{1-x}As$ superlattice showed that when the electron energy is comparable to potential barrier height, narrow passbands and/or broad stopbands can be obtained when the unit cell is divided into four or more sublayers. The bandgap can also be adjusted through changing the total volume ratio of $Al_xGa_{1-x}As$ and GaAs in one unit cell. When the ratio of $Al_xGa_{1-x}As$ to GaAs increases, narrower passbands can be obtained and each passband also moves to higher energy. Another design of quantum well/barrier structure is to combine two sub-superlattices of different periods with each unit cell containing six sublayers of alternating GaAs and $Al_xGa_{1-x}As$. Two very narrow passbands were obtained in the vicinity of the barrier height V_0. Our results showed that it is possible to produce high-Q electron energy filters with narrow peaks of transmission coefficient using quantum well/barrier superlattices with unit cells containing substructures. Experimentally, photoreflectance spectroscopy is an accurate method for the characterization of multiple-quantum-well structures [17]. It is would be interesting to verify our theoretical results using this technique.

References

[1] D. Chemla, A. Pinczuk, IEEE J. Quant. Electron. 22 (1986) 1609.
[2] T. Ando, A.B. Fower, F. Stern, Rev. Mod. Phys. 54 (1982) 437.
[3] B. Ricco, M.Y. Azbel, Phys. Rev. B 29 (1984) 1970.
[4] R.M. Kolbas, N. Holonyak, Jr, Am. J. Phys. 52 (1984) 431.
[5] F.Y. Huang, Appl. Phys. Lett. 57 (1990) 2199.
[6] L. Esaki, in: L.L. Chang, B.C. Beissen (Eds.), Synthetic Modulated Structures, Academic Press, New York, 1985.
[7] P.L. Wang, S.J. Xiong, Phys. Rev. B 49 (1994) 10373.
[8] P. Cusumano, B.S. Ooi, A. Saher Helmy, S.G. Ayling, A.C. Bryce, J.H. Marsh, B. Voegele, M.J. Rose, J. Appl. Phys. 81 (1997) 2445.
[9] X.S. Chen, X.Q. Liu, W. Liu, S.C. Shen, A. Sasaki, J. Appl. Phys. 85 (1999) 7797.
[10] M.R. Shen, W. Cao, Appl. Phys. Lett. 75 (1999) 3713.
[11] R. De, L. Kronig, W.G. Penny, Proc. Roy. Soc. A 130 (1931) 499.
[12] A. Elci, Phys. Rev. B 34 (1986) 8616.
[13] W.L. Bloss, Phys. Rev. B 44 (1991) 8035.
[14] P.T. Landsberg, IEEE J. Quant. Electron. 21 (1985) 434.
[15] G. Basterd, Phys. Rev. B 24 (1981) 5693.
[16] W. Cao, W.K. Qi, J. Appl. Phys. 78 (1995) 4627.
[17] G.F. Lorusso, F. Tassone, V. Capozzi, C. Perna, D. Martin, Solid State Commun. 98 (1996) 705.